Soil management for sustainable agriculture under climate change

A modelling study

Mario Feifel

Independent project • 30 credits
Swedish University of Agricultural Sciences, SLU
Faculty of Natural Resources and Agricultural Sciences, Department of Soil and Environment
EnvEuro - European Master in Environmental Science
Examensarbeten/Institutionen för mark och miljö, SLU
Part number 2024:18
Uppsala 2024

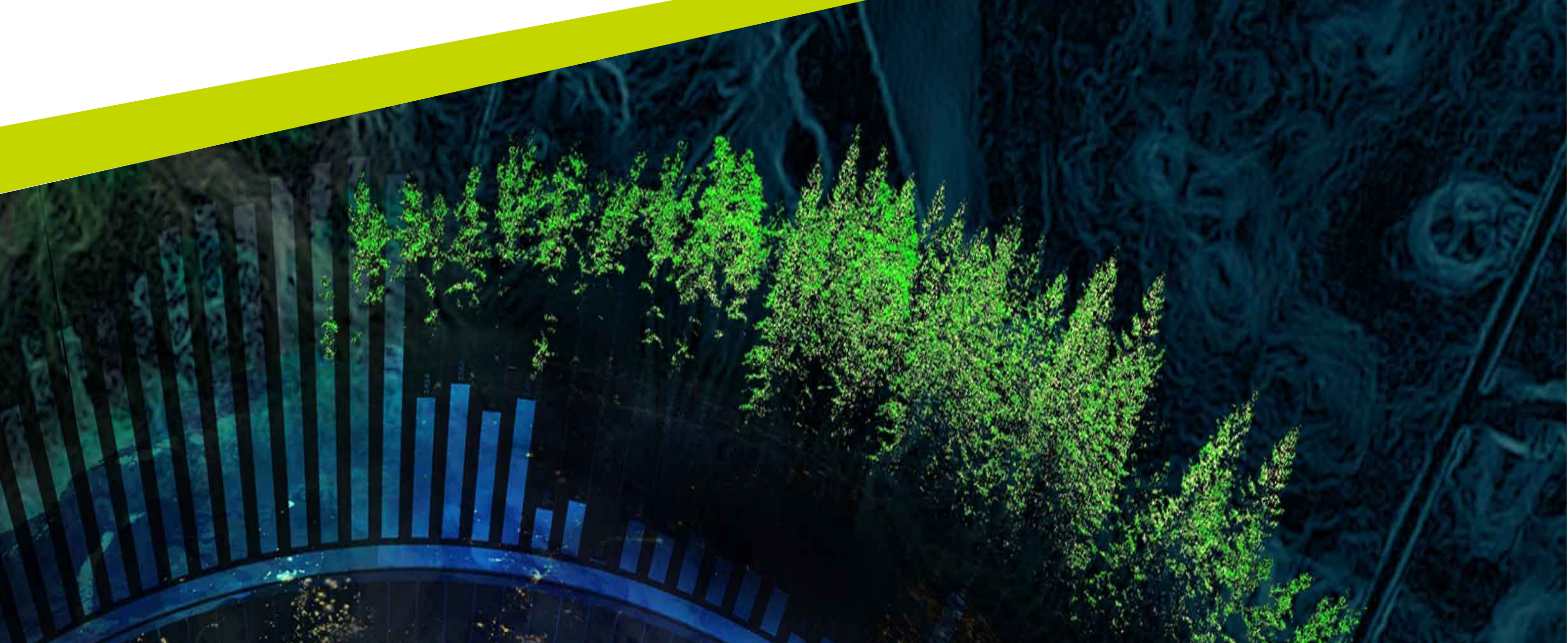

Soil management for sustainable agriculture under climate change. A modelling study.

Mario Feifel

Supervisor:	**Nicholas Jarvis, Swedish University of Agricultural Sciences, Department of Soil and Environment**
Assistant supervisor:	Elsa Coucheney, Swedish University of Agricultural Sciences, Department of Soil and Environment
Assistant supervisor:	Sebastian Gayler, University of Hohenheim, Department of Biogeophysics
Examiner:	Mats Larsbo, Swedish University of Agricultural Sciences, Department of Soil and Environment

Credits:	30
Level:	A2E
Course title:	Master thesis in Environmental science
Course code:	EX0897
Programme/education:	EnvEuro - European Master in Environmental Science
Course coordinating dept:	Department of Soil and Environment
Place of publication:	Uppsala
Year of publication:	2024
Copyright:	All featured images are used with permission from the copyright owner.

Keywords:	Conservation agriculture, no-till farming, soil-crop-model, soil organic matter, soil structure.

Swedish University of Agricultural Sciences

Faculty of Natural Resources and Agricultural Sciences

Department of Soil and Environment

Soil and Environmental Physics

Abstract

Conservation agriculture practices, such as reduced tillage or residue retention, have gained attention for their potential to enhance agricultural system resilience to climate change and combat soil degradation. However, conventional soil-crop models often neglect the dynamics of soil properties, limiting their ability to predict changes in soil quality on large timescales relevant for sustainable management.

This study therefore applies and expands the recently developed Uppsala model of Soil Structure and Function to investigate the long-term impacts of conservation agriculture on soil organic matter (SOM) stocks, the water balance and winter wheat yields under current and future climate in temperate Europe.

The model was calibrated for a site in Switzerland and used to simulate a baseline period (1985-2015) as well as 6 future climate change scenarios (2020-2090) under two contrasting soil managements. Conventional intensive tillage with residue incorporation (CIT) was compared to no-till practices with residue retention (CNT).

Under current climate conditions, the CNT treatment was able to conserve soil moisture by reducing surface runoff (-97 %) and evaporation (-65 %), as compared to CIT. Though yields remained similar, as under the wet climate, crop growth was not limited by water availability. After 30 years, SOM stocks were 2.8 % higher under CIT, due to larger amounts of above-ground biomass being incorporated through tillage. In future climate projections, significant yield declines were simulated under hotter conditions, driven by much shorter growing periods, potentially linked to limitations of the employed phenology model. Despite declining SOM levels in both systems, CNT maintained 14% higher SOM on average.

Although no-till practices did not enhance yields, they showed strong potential to mitigate climate change impacts on SOM and soil function. This suggests that no-till practices, together with adequate residue management, could be a promising strategy for sustaining soil quality in the face of climate change. Further model development and improvement is necessary to predict the long-term effects on grain yields.

Keywords: Conservation agriculture, no-till farming, soil-crop-model, soil organic matter, soil structure

Table of contents

List of tables

List of figures

Abbreviations

CIT	Conventional intensive tillage
CNT	Conventional no tillage
FAST	Farming System and Tillage Experiment
GLUE	Generalized likelihood uncertainty estimation
LAI	Leaf area index
NSME	Nash-Sutcliff Model efficiency
OIT	Organic intensive tillage
ORT	Organic reduced tillage
SOM	Soil organic matter
SSP	Shared socioeconomic pathway
USSF	Uppsala model of Soil Structure and Function

1. Motivation and aims of the study

Agricultural production in Europe is already affected by climate change in various ways (EEA, 2019). The frequency and intensity of extreme weather events is expected to rise further, posing an increasing challenge to meet food production demands in the future (IPCC, 2023). Meanwhile, 60-70 % of European soils are unhealthy and are continuously degrading (European Commission, 2020b).

Two commonly discussed adaptation strategies that aim to improve soil health are a reduction in tillage intensity and the use of plant residues for soil cover (FAO, 2017). Conservation agriculture in particular has gained attention for its potential benefits in soil structure improvement, water retention, and possibly carbon sequestration (Verhulst et al., 2010, Palm et al., 2014). Conservation farming combines reduced tillage or no-till farming systems with permanent crop and residue cover as well as crop rotations, aiming to minimize soil disturbance, maintain soil aggregates, reduce surface runoff and evaporation, and enhance the organic matter content in the topsoil. These factors may contribute to improve soil quality and water use efficiency, helping to maintain or potentially even increase crop yields in the future (Scopel et al., 2013).

In order to accurately predict long-term effects of both agricultural management and climate change on soil quality and future crop yields, it is necessary to develop and improve soil-crop simulation models that describe the temporal variation of soil properties (Strudley et al., 2008). Common soil-crop models often treat the soil as a static object with time-constant hydraulic properties and are therefore unable to capture changes on longer time scales (years to decades) that are relevant for sustainable soil management (Jarvis et al., 2024).

The recently developed Uppsala model of Soil Structure and Function (USSF) was designed to fill that gap (Jarvis et al., 2024). USSF has been shown to realistically simulate the effects of long-term organic amendments in the restoration of degraded soils, but it is currently unable to model different residue management practices related to conservation agriculture. This study therefore introduces a simple residue module to USSF to predict the influence of decomposing surface residues on the surface water fluxes, soil temperature regulation, anecic earthworm burrowing and organic matter incorporation.

In order to examine the effects of different tillage and residue management systems on soil properties and crop yields under future climates in temperate Europe, the USSF model was first calibrated using data from an agricultural site near Zürich, Switzerland. Then, scenario simulations were conducted, by applying two contrasting management systems (conventional tillage with residue incorporation and no-till with surface residues) to a continuous winter wheat crop. After simulating a 30-year baseline scenario with recorded weather data, 18 future climate scenarios were calculated, analysed and compared. The aim was to evaluate the long-term positive and negative effects of management practices related to conservation agriculture on crop growth and yields, soil structure, soil organic matter (SOM) dynamics and the water balance.

2. Methods

2.1 Site description and experimental data

Experimental data were collected at the long-term “Farming System and Tillage Experiment (FAST)” at N47.4389° E8.5278° in 8153 Rümlang, Switzerland in 2019 (Agroscope, 2021; Prechsl et al., 2017; Wittwer et al., 2017). The site is located 485 m above sea level and experiences an average of 1050 mm precipitation per year at a mean air temperature of 9.4 °C. Four different treatments are being examined on the site. A conventional farming system using mineral fertilizers and synthetic plant-protection products is combined with both intensive tillage (CIT) and no-till (CNT). Two additional treatments combine organic farming practices using organic fertilizers and no additional plant-protection products with intensive tillage (OIT) and reduced tillage (ORT). The experimental design makes use of four blocks (A-D) where block A is of another soil type than B-D. A six-year crop rotation consists of winter wheat, maize, legumes, winter wheat and temporary ley (2 years).

This study focuses only on the conventional systems (CIT and CNT) of the blocks B-D for a winter wheat crop sown on October 25th 2018 and harvested on July 23rd 2019. In this period, 3-4 replicate measurements of leaf area index (LAI) were made for each treatment and block every 7-10 days from April through June. Additionally, harvested grain and above-ground residue biomass were measured after harvest. Water contents at depths of 0.10 m and 0.40 m were continuously monitored in the blocks B and C, respectively, from April through July 2019. No replicates were made for the water content measurements. The soil type is an endostagnic Cambisol with a loamy texture. A profile description can be found in Table A1. Additionally, data on soil water retention (HYPROP) and unsaturated hydraulic conductivities (tension infiltrometer) were available for the site and were used to parameterize parts of the model.

The water contents measured at 0.40 m depth in the no-till treatment diverged considerably from the measurements in the other three treatments, whereas those measured at 0.10 m depth were similar in all treatments. We could not explain this behaviour based on our knowledge of the site and the treatments and suspected that this has been caused by local heterogeneities in soil texture or problems with the sensor. These measurements were therefore excluded from further analysis.

Phenological observations at a nearby site in 8052 Seebach, Switzerland were used to calibrate the crop phenology model. The recorded data were obtained as part of the official Swiss variety trials (Watroba & Levy Häner, 2021) and included dates of sowing, flowering and harvest for 12 different years of winter wheat cultivation between 2008 and 2020.

2.2 The USSF model

The Uppsala model of Soil Structure and Function (USSF) is a recently developed soil-crop-model that aims to capture long-term effects of land use and climate change on soil quality and crop production by accounting for the dynamics of soil structure and soil hydraulic properties (Jarvis et al., 2024). USSF therefore combines three main modules (crop growth, soil water and organic matter dynamics) to describe the stocks and flows of water and organic matter within the soil-plant-atmosphere-continuum on a seasonal to decadal timescale.

The existing model was extended by a new module describing decaying crop residues at the soil surface and how they affect the upper boundary condition of the modelled soil column. This was necessary to address the effects of no-till management practices on water and organic matter cycling. The following sections describe the parts of the USSF model most relevant to the present study (i.e., crop phenology, organic matter allocation in the soil, and soil structure dynamics), as well as the newly introduced functions (i.e., surface residues, ponding). The nomenclature utilized in this study was adopted from Jarvis et al. (2024).

2.2.1 Soil water flow and soil structure dynamics

USSF applies Richards' equation to calculate water flow within the soil and across the profile boundaries. The matric potential at the base of the profile is assumed to be in hydrostatic equilibrium with the groundwater. The groundwater depth follows an annual sinusoidal variation based on a minimum and a maximum depth as well as the date of the maximum.

The water retention and hydraulic conductivity characteristics in USSF are obtained by combining the Brooks-Corey-Mualem model (Brooks & Corey, 1964; Mualem, 1976) with the model described by Jarvis (2008) for near-saturated macropore retention and conductivity. In particular, the model continuously estimates the porosity, pore size distribution index and saturated hydraulic conductivity in both the macropore and the mesopore region. This is achieved by coupling to a model that describes the dynamics of the soil pore space, as influenced by tillage and subsequent consolidation, SOM dynamics, and crack formation during shrinkage due to soil drying.

To simulate SOM dynamics, USSF employs the dual-porosity version of the ICBM model (Andrén & Kätterer, 1997; Meurer et al., 2020; Coucheney et al., 2024). SOM is split into four pools with different properties according to their age (young or old) and their respective location in the pore space (stored in micropores or in mesopores). Total SOM amount and its allocation to the pore size classes affect the pore size distribution both directly and indirectly. For example, micro- and mesoporosity are a function of SOM contents and the share of SOM stored in the respective pore region, while for bio(macro)porosity generation USSF indirectly utilizes SOM contents to estimate soil faunal activities. The pore size distribution in turn affects soil hydraulic properties as outlined above.

2.2.2 Crop growth

The following section briefly describes the model processes and functions related to crop development, root growth and grain production that are relevant to this study. For a more detailed description, see Jarvis et al. (2024).

Phenological development

Crop growth is simulated by estimating the dry matter assimilation from photosynthesis, by applying the concept of radiation use efficiency, and its subsequent allocation to various plant organs. The allocation fractions for roots, leaves, stem and grain $\left(f_{root}, f_{leaf}, f_{stem}, f_{grain}\right)$ [-] are dependent on the development stage S_d [-] of the crop, which in turn is a function of the temperature sum T_{sum} [°C d] after the sowing date of the crop:

$$T_{sum} = \sum \left(\max \left(0; \frac{T_{max} - T_{min}}{2} - T_b \right) * f_{vern} \right) \quad (1)$$

where T_{max} and T_{min} [°C] are the minimum and maximum daily air temperatures measured at a height of 2 meters, T_b [°C] is a crop specific base temperature and f_{vern} [-] is a factor accounting for the vernalization requirements of winter crops, as described in Ceglar et al. (2019).

The development stage is then given by:

$$S_d = \begin{cases} 0 & ; T_{sum} \leq T_{sum(e)} \\ \frac{T_{sum} - T_{sum(e)}}{T_{sum(a)} - T_{sum(e)}} & ; T_{sum(e)} < T_{sum} \leq T_{sum(a)} \\ 1 + \frac{T_{sum} - T_{sum(a)}}{T_{sum(m)} - T_{sum(a)}} & ; T_{sum(a)} < T_{sum} \leq T_{sum(m)} \\ 2 & ; T_{sum} > T_{sum(m)} \end{cases} \quad (2)$$

where $T_{sum(e)}$, $T_{sum(a)}$ and $T_{sum(m)}$ [°C d] are the temperature sums required to reach crop emergence, anthesis and maturity respectively.

All phenological parameters except the required temperature sums were set to the default values for winter wheat in the SWAP Model (Kroes et al., 2017). The temperature sums $T_{sum(e)}$, $T_{sum(a)}$ and $T_{sum(m)}$ [°C d] were derived from phenological observations and recorded wheather data and are shown together with the other phenological parameters in Table A2.

Root growth

USSF mimics root growth by applying a diffusion model to the root biomass:

$$\frac{\partial B_{root}}{\partial t} = \frac{\partial}{\partial z}\left(D\left(\frac{\partial B_{root}}{\partial z}\right)\right) - I_r \quad (3)$$

where B_{root} [kg m^{-2}] is the dry root biomass in a given soil layer, t [d] is time, z [m] is depth, D [m^2 d^{-1}] is the root diffusion coefficient and I_r [kg m^{-2} d^{-1}] is the root decay rate.

The input of root biomass is modelled as an upper boundary flux to the diffusion equation, while the lower boundary conditions is assumed to be zero flux. The amount of biomass allocated to roots is limited either by the potential root growth rate or the supply of assimilates to the roots. Hereby, the maximum fraction of assimilates allocated to the roots is dependent on the development stage.

Grain filling

After maturity, during the later stages of crop development, assimilates are increasingly allocated to the grain. Additionally, biomass is also translocated within the plant from both stem reserves and green leaves during senescence. The change in dry grain biomass B_{grain} [kg m^{-2}] is therefore given by:

$$\frac{dB_{grain}}{dt} = f_{grain}A + \Gamma_{\mathrm{d3}} k_{tr} B_{stem} + \Gamma_{\mathrm{d2}} f_{tr} k_{sen} B_{leaf(g)} - \Gamma_{\mathrm{h}} B_{grain} \quad (4)$$

where A [kg m^{-2} d^{-1}] is the total dry matter assimilation rate by the crop, Γ_{d2} and Γ_{d3} are binary variables indicating whether the respective development stage has been reached or not (unity or zero), k_{tr} [d^{-1}] is a translocation rate constant for the transfer of stem reserves to the grain, B_{stem} [kg m^{-2}] and $B_{leaf(g)}$ [kg m^{-2}] are the dry stem and dry green leaf biomass and Γ_h is a binary variable indicating whether harvest occurs or not (unity or zero).

2.2.3 Model Development: A new surface residue module

With the aim to perform long-term simulations of different tillage systems, adaptations had to be made to the original USSF model. One positive effect of no-till practices is moisture conservation through improved infiltration and decreased evaporation. This was not accounted for in the original model, since crop residues were immediately incorporated at harvest. Consequently, a surface residue module was introduced. This module comprises routines to calculate surface residue decomposition rates, tillage- and bio-incorporation of surface residues into the soil, bioporosity generation by earthworm burrowing, surface radiation cover and heat insulation.

Crop residue dynamics at the soil surface

The change in surface residue biomass B_{res} [kg m^{-2}] is given by:

$$\frac{dB_{res}}{dt} = \left(\left(1 - f_{export}\right)\Gamma_h B_{ag}\right) - \left(k_{res}k_{t(res)}B_{res}\right) - \left(\Gamma_d B_{res}\right) \tag{5}$$

where B_{ag} [kg m^{-2}] is the mass of above-ground harvest residues and f_{export} [-] is the proportion of residues exported at harvest, k_{res} [d^{-1}] is a first-order rate constant for the decay of residue biomass, $k_{t(res)}$ [-] is a temperature response function regulating the decomposition rate and Γ_d is a binary variable indicating whether tillage occurs or not (unity or zero).

The inputs of residue biomass to the SOM pool through bio-incorporation $I_{a(bio)}$ [kg m^{-2} d^{-1}] and by tillage $I_{a(d)}$ [kg m^{-2} d^{-1}] are given by:

$$I_{a(bio)} = f_{inc(bio)}f_{ret}\left(k_{res}k_{t(res)}B_{res}\right) \tag{6}$$

$$I_{a(d)} = f_{inc(d)}\left(\Gamma_d B_{res}\right) \tag{7}$$

where f_{ret} [-] is the fraction of residue biomass that is retained (not respired) during decomposition, while $f_{inc(bio)}$ [-] and $f_{inc(d)}$ [-] are the proportions of the organic matter that enter a certain soil layer, during bio-incorporation and tillage, respectively. Here, f_{ret} was set to the same value (0.35) as the corresponding microbial efficiency parameter used in SOM decomposition, based on the parameterization in Coucheney et al. (2024). The depth distribution for bio-incorporation is a user-specified exponential function, which distributes organic matter between the soil surface and the maximum depth of anecic earthworm burrowing z_{max} [m]. The distribution of organic matter during a tillage event is assumed uniform within the tillage depth. All incorporated crop residues are allocated to the young organic matter pool in the mesopore region.

Generation of bioporosity

The effects of surface residue availability on anecic earthworm burrowing activity are approximated by a linear relationship between bioporosity generation and surface residue biomass:

$$\tau_a = f_{bio_a} \max(\tau_{a_0}; \alpha_{bio} B_{res}) \tag{8}$$

where τ_a [m^3 m^{-3} d^{-1}] is the rate of bioporosity formation due to anecic earthworms, f_{bio_a} [-] is the proportion of bioporosity generated in the respective soil layer (assuming a uniform distribution within the maximum depth of earthworm burrowing), α_{bio} [m^3 m^{-3} d^{-1} (kg m^{-2})$^{-1}$] is the rate of bioporosity generated per amount of surface residue and τ_{a_0} [m^3 m^{-3} d^{-1}] is the minimum rate of bioporosity generated in the absence of residues at the soil surface. The latter parameter is used to compensate for the fact that litter fall is not explicitly modelled in USSF and thus residue availability is underestimated during the growing season.

Partitioning between transpiration and evaporation

Surface residues provide cover for the soil surface through shading and aerodynamic resistance to heat and vapor flow, thereby reducing potential evaporation and buffering soil temperature extremes. The fraction of solar radiation intercepted by crop residues $f_{int(res)}$ [-] is given by the following linear relationship:

$$f_{int(res)} = \min\left(1, \frac{B_{res}}{B_{crit}}\right) \tag{9}$$

where B_{crit} [kg m^{-2}] is the critical residue biomass, when complete soil cover is reached.

The residue cover fraction is used in the partitioning of potential evapotranspiration ET_p [m d^{-1}] into transpiration T_p [m d^{-1}] and evaporation from the soil surface $E_{s,p}$ [m d^{-1}]:

$$T_p = f_{int(green\ leaf)} ET_p \tag{10}$$

$$E_{s,p} = \left(1 - f_{int(leaf)}\right)\left(1 - f_{int(res)}\right) ET_p \tag{11}$$

where $f_{int(green\,leaf)}$ [-] and $f_{int(leaf)}$ [-] are the fractions of solar radiation intercepted by green leaves and the full canopy, respectively. Consequently, higher surface cover by residues reduces the potential soil evaporation rate without affecting potential transpiration.

Surface ponding

Surface residues are also able to reduce run-off by generating a mechanical resistance to flowing surface water and increasing its flow path. Ponding has so far not been accounted for in USSF, as all non-infiltrating water was assumed to generate immediate run-off. Here, a simple approach is introduced to approximate the effects of crop residues on re-infiltration and run-off as well as interception.

The change in depth of the ponded water column V_{pond} [m] can be expressed as:

$$\frac{dV_{pond}}{dt} = q_{in} - q_r - q_{reinfil} \tag{12}$$

where q_{in} [m d^{-1}] is the sum of all inflows to the pond from the atmosphere, q_r [m d^{-1}] is the surface run-off rate and $q_{reinfil}$ [m d^{-1}] is the reinfiltration rate.

Inflow to the pond occurs only when the infiltration capacity I_{cap} [m d^{-1}], calculated from Darcy's law, is surpassed by precipitation and snowmelt:

$$q_{in} = \max(0;\ P - S_f + S_m - I_{cap}) \tag{13}$$

where P [m d^{-1}] is the precipitation rate, and S_f and S_m [m d^{-1}] are the snowfall rate and the melting rate of the snowpack.

The run-off rate is expressed as a function of the depth of the ponded water column:

$$q_r = \max\left(0;\ \frac{V_{pond} - V_{max}}{dt}\right) \tag{14}$$

where V_{max} [m] is the maximum depth of ponded water that can be held by surface residues before run-off is generated, given by:

$$V_{max} = \beta_{res} B_{res} \tag{15}$$

Where β_{res} [m^3 kg^{-1}] is the specific water holding capacity of crop residues.

The reinfiltration rate of ponded surface water into the soil is given by the remaining infiltration capacity I_{cap} [m d^{-1}] after infiltration has taken place:

$$q_{reinf} = \min\left(I_{cap} - q_0\ ;\ \frac{V_{pond}}{dt}\right) \tag{16}$$

where q_0 [m d^{-1}] is the infiltration rate of rain and meltwater.

While surface residues can reduce run-off and soil evaporation, they can also decrease net infiltration by intercepting some precipitation during rainfall. This was implemented indirectly by allowing water to evaporate from the fraction of the soil surface that is covered by residues $f_{int(res)}$ during periods when the residues are assumed to be wet (i.e., during rain events and snowmelt or if there is any ponded surface water after a precipitation event). Otherwise, the residue layer is assumed to be dry.

$$E_{r,p} = \begin{cases} \left(1 - f_{int(leaf)}\right) f_{int(res)}\ ET_{pot}, & \text{if } \left(P - S_f + S_m > 0\right) \vee \left(V_{pond} > 0\right) \\ 0 & \text{, if } \left(P - S_f + S_m = 0\right) \wedge \left(V_{pond} = 0\right) \end{cases} \quad (17)$$

$$E_{r,a} = \min\left(\frac{V_{pond}}{dt}; E_{r,p}\right) \quad (18)$$

where $E_{r,p}$ and $E_{r,a}$ [m d^{-1}] are the potential and the actual evaporation rate from the residue layer.

Because residue water contents are not explicitly described, residue evaporation is assumed to take place from the first soil layer, instead of the residue layer. In the case of ponding, the water evaporated from the soil surface is immediately replenished from the pond by reinfiltration.

This changes the equation for upper boundary water flux $q_{upperBC}$ [m d^{-1}] to:

$$q_{upperBC} = E_{s,a} + E_{r,a} - q_0 - q_{reinfil} \quad (19)$$

where $E_{s,a}$ [m d^{-1}] is the actual soil evaporation rate.

Soil surface temperature

The soil surface temperature T_{surf} [°C] under both snow and residue cover is approximated using a weighted average of the current air temperature T_{air} [°C] and the midpoint-temperature of the uppermost soil layer T_{soil} [°C]:

$$T_{surf} = \frac{\left(D_{soil} D_{snow} {z_{res}}^2 + D_{soil} D_{res} {z_{snow}}^2\right) T_{soil} + D_{res} D_{snow} \frac{\Delta z^2}{2}\ T_{air}}{D_{soil} D_{snow} {z_{res}}^2 + D_{soil} D_{res} {z_{snow}}^2 + D_{res} D_{snow} \frac{\Delta z^2}{2}} \quad (20)$$

where D_{soil}, D_{snow} and D_{res} [m^2 d^{-1}] are the thermal diffusivities of the uppermost soil layer, the snow layer and the residue layer, respectively and Δz, z_{snow} and z_{res} [m] are the thicknesses of these three layers. Note that when the soil surface is covered neither by snow nor crop residues ($z_{snow} = z_{res} = 0$), this simplifies to:

$$T_{surf} = T_{air} \quad (21)$$

The relationship between the residue biomass and the residue layer thickness is given by the assumption of a constant residue bulk density ρ_{res} [kg m^{-3}] (Gonzalez-Sosa et al., 2001):

$$z_{res} = \frac{B_{res}}{\rho_{res}} \tag{22}$$

2.3 Model calibration

The model was set up for the FAST site using the available information on the soil profile, texture, SOM and soil hydraulic properties. Crop phenology parameters of winter wheat were estimated to match observations from the Swiss crop variety trials conducted over 12 years at a nearby site in Seebach, Zürich, Switzerland. Any remaining model parameters that were not subject to the model calibration were set to the USSF default values or chosen according to literature and previous calibrations to a site in Ultuna, Uppsala, Sweden (Jarvis, 2024; Coucheney et al., 2024). The calibration simulations were run for 277 days from sowing until harvest of the winter wheat crop (25th October 2018 – 26th July 2019), for which daily minimum and maximum air temperatures as well as hourly precipitation data were retrieved from MeteoSwiss, the Federal Office of Meteorology and Climatology of Switzerland (MeteoSwiss, 2024).

GLUE analysis and selection of parameter sets

A generalized likelihood uncertainty estimation (GLUE; n = 5000 sets) procedure was carried out for both treatments in order to identify acceptable parameter sets for 7 uncertain crop parameters and the maximum groundwater depth (Beven & Binley, 1992). The model parameters and their ranges used in the GLUE analysis can be found in Table 1.

5000 parameter sets were generated by randomly drawing 8 parameter values from uniform distributions within their respective ranges. These 5000 parameter sets were used to run independent simulations, and the results were then compared against the field measurements for both treatments. Two likelihood measures were used for the different target variables. First, the Nash-Sutcliff Model Efficiency (NSME) was calculated for observed leaf area indices and measured water contents at 0.10 m and 0.40 m depth (Nash & Sutcliffe, 1970):

$$NSME = \frac{\sum_{i=1}^{n}(O_i - \bar{O})^2 - \sum_{i=1}^{n}(O_i - P_i)^2}{\sum_{i=1}^{n}(O_i - \bar{O})^2} \tag{23}$$

where O and P are the observed and predicted values of a given variable, $\bar{O}$ is the mean value of the observations and n is the number of observations.

Additionally, the absolute errors (AE) of grain yield and above-ground residue biomass were used as a second measure.

$$AE = |O_i - P_i| \tag{24}$$

Table 1: Model parameters used in the GLUE analysis.

Parameter	Description	Range	Unit
D_{max}	maximum value of the root diffusion coefficient	5.0 - 20.0	$cm^2\ d^{-1}$
$f_{bg(max,e)}$	maximum fraction of dry matter allocated below-ground (to roots and root exudates) in the early stages	0.4 - 0.8	-
$f_{leaf(max)}$	maximum fraction of dry matter allocated to the leaves	0.3 - 0.6	-
$k_{sen(min)}$	minimum leaf senescence rate coefficient	0.02 - 0.04	d^{-1}
k_{tr}	translocation rate constant determining the rate of transfer of reserves stored in the stem to the grain	0.002 - 0.010	d^{-1}
$R_{bg(pot)}$	potential root growth rate coefficient	0.1 - 0.3	d^{-1}
RUE_{max}	maximum solar radiation use efficiency	1.3 - 1.8	$g\ MJ^{-1}$
GW_{max}	maximum groundwater depth assuming an annual sinusoidal variation	2.0 - 3.5	m

2.4 Climate scenarios

To predict long-term changes in crop production, SOM stocks and soil structure under current and future climate, simulations were run on a 30-year baseline period and 18 future climate projections for the years 2020-2090. For the baseline period, weather data recorded between 1985 and 2015 were used (MeteoSwiss, 2024). In the future scenarios, three different climate models (Table 2) and two Shared Socioeconomic Pathways (SSP 2-4.5 and SSP 5-8.5; IPCC, 2023) were selected from the CMIP6 ensemble (Copernicus Climate Change Service, 2021) to cover a wide variety of possible climate projections. For each model, 3 realizations of transient projections of daily precipitation, air temperatures and solar radiation were used, representing the 10^{th}, 50^{th}, and 90^{th} precipitation percentiles of in total 50 realizations that were obtained using the LARS-WG weather generator (Semenov & Barrow, 2002).

Table 2: Underlying models for the future climate scenarios.

Climate model	Full name	Main reference
CNRM-CM6	Centre National de Recherches Meteorologiques - Climate Model Version 6	(Voldoire et al., 2019)
MRI-ESM2-0	Meteorological Research Institute - Earth System Model version 2	(Yukimoto et al., 2019)
UKESM1-0-LL	UK Met Office Earth System Model version 1.0	(Sellar et al., 2019)

Rainfall disaggregation

Climate variables required in USSF are daily minimum and maximum temperatures as well as daily or subdaily precipitation data. The employed climate scenarios only had daily resolution, but the precipitation projections were disaggregated into subdaily intervals in order to better capture effects of the high intensity rainfall events that are expected to become more common in the future.

A method described by Olsson (1998) and later modified by Güntner et al. (2001) was further modified in the present study and subsequently applied to increase the resolution of the rainfall data from one day to 45 minutes. The model is a random cascade applying the following generator:

$$W_1, W_2 = \begin{cases} 0, 1 & \text{with } P(0|1) \\ 1, 0 & \text{with } P(1|0) \\ W_{x/x}, 1 - W_{x/x} & \text{with } P(x|x) \end{cases} \tag{25}$$

with $0 < W_{x/x} < 1$

and $P(0|1) + P(1|0) + P(x|x) = 1$

where W_1 and W_2 are the weights used for the branching of a wet box, $W_{x/x}$ is an empirical distribution, and $P(0|1)$, $P(1|0)$, and $P(x|x)$ are the probabilities of the respective branching division.

The model weights and probabilities were calibrated to on-site hourly precipitation data from 1981-2024 (MeteoSwiss, 2024). However, instead of using theoretical distribution functions (Olsson, 1998) or seven-interval histograms (Güntner et al., 2001), the exact empirical distribution retrieved from the calibration period was used for $W_{x/x}$. Both the weights and probabilities derived from the calibration were in agreement with those found in previous calibrations (Güntner et al., 2001; Olsson, 1998).

The calibrated rainfall generator was then applied to the climate projections to disaggregate the daily precipitation into 45-minute intervals.

3. Results & Discussion

3.1 Calibration

Of the 5000 tested parameter sets, acceptable sets were selected as follows:

1. The simulated grain yields and residue biomass must be within 2 standard deviations of the observed means (5.8 ± 1.4 and 7.9 ± 2.0 t ha^{-1}, respectively). Here, a trade-off was observed, where either LAI was underestimated, or grain and residue biomasses were overestimated. This was to be expected, since nutrient deficiency, weeds or pests were neglected in the simulation, which means that the model predicted water-limited potential yields that cannot always be achieved in reality.

2. From the parameter sets fulfilling the first conditions, the best 10 sets were chosen according to their NSME for leaf area index. Since the NSMEs for the water content predictions were poor and varied to a small extent, they were not used in the selection of the final parameter sets.

3. To identify any unexpected behaviour in a long-term simulation, these 10 parameter sets were then tested on the 30-year baseline period. The results showed that under current climate conditions all tested parameter sets performed satisfactorily in simulating water balance, LAI, harvest index and root-to-shoot ratio.

4. A final selection of 3 parameter sets was chosen manually from the best 10 sets to maximize parameter variability, i.e., to avoid sets with similar parameter values (Table 3).

Table 3: Final parameter sets used in the climate projections.

D_{max}	$f_{bg(max,e)}$	$f_{leaf(max)}$	$k_{sen(min)}$	k_{tr}	$R_{bg(pot)}$	RUE_{max}	GW_{max}
cm^2 d^{-1}	-	-	d^{-1}	d^{-1}	d^{-1}	g MJ^{-1}	m
5.6	0.73	0.59	0.038	0.0050	0.11	1.38	2.57
8.2	0.49	0.44	0.039	0.0053	0.21	1.36	2.19
15.2	0.59	0.54	0.038	0.0044	0.13	1.30	2.29

3.2 Baseline simulations

Crop performance

During the baseline period (1985 - 2015), simulations were carried out with the 10 best parameter sets for both the intensive tillage and the no-till treatment. Figure 1 shows the simulated grain yields, above-ground residues and peak LAI for the 3 final parameter sets for the baseline period, as well as the average winter temperatures.

The average simulated annual grain yield across both treatments and all parameter sets was 6.2 t ha^{-1}. The differences between parameter sets were larger than those between treatments. The first parameter set generally showed a high inter-annual variability in grain yield and residue biomass as well as LAI. Meanwhile, the other two sets were more stable from year-to-year. Simulated peak LAI was rather low with an overall average value of 3.5 m^2 m^{-2}, but with significant variations during the baseline period, taking values between 1.9 and 6.1 m^2 m^{-2}. Grain yield, residue biomass and LAI all showed a strong inverse relationship with the average air temperatures in the winter months, with poor crop performance following a warm winter and better performance after a cool winter.

The high sensitivity to winter temperatures is a consequence of the representation of crop phenology in the model. The simple approach of calculating crop development rates solely from growing degree days gave highly fluctuating crop development rates in the different years. In the baseline period, the day of flowering (development stage = 1) ranged from 10th May in 2007 to 25th June in 1987 (46 days), while the observed range of flowering dates used in the calibration of the temperature sums (12 years between 2008 and 2020) was only 21st May to 10th June (20 days). It has been noted before that phenology models which are linearly dependent on temperature sums have a tendency to overestimate development rates during high temperature anomalies (Ceglar et al., 2011). An accelerated phenology shortens the duration of the growth period and consequently reduces biomass assimilation and yields (Craufurd & Wheeler, 2009). This has also been found in experimental studies (e.g., Wheeler et al., 1996). An overestimation of phenological development rates in the model therefore likely causes an underestimation of simulated LAI and yields in years with warm winters. Despite LAI and yields being low, they still varied within reasonable ranges, compared to the available measurements.

SOM stocks

After small decreases from the initial conditions within the first 5 - 10 years the SOM stocks in the profile remained relatively stable during the baseline period for both treatments and all three crop parameter sets (Figure 2A). Interestingly, in the last year of the baseline period, the CIT treatments had on average 2.8 % larger SOM stocks than CNT. While SOM mineralization rates were higher in the CIT treatment, the total incorporation of crop residues into the soil was also larger, because the earlier incorporation during tillage mitigated losses by accelerated decomposition at the surface (Table 4). The CIT treatment exhibited a uniform distribution of SOM throughout the tilled layer (0 - 0.2 m), whereas under CNT, the SOM became stratified, with higher contents in the uppermost 0.05 m and lower contents below (Figure 2B). Below 0.25 m there were only small differences in SOM content between the treatments. Furthermore, the annual variation in SOM stock was higher for the CIT treatment, with a sharp increase in SOM following the tillage incorporation but also a steeper decrease in the summer months, as compared with the CNT treatment.

After the first 10 simulated years, all simulated parameter sets and both tillage treatments were in quasi-steady state. Any differences in the total stock of SOM between the treatments were only due to differences within the uppermost soil layers affected by tillage. This is also reflected in the amplitude of annual variation of SOM, where tillage incorporation temporarily increases SOM stocks in the CIT treatment, but this gain is partially lost throughout the year, due to accelerated mineralization. The loss of protection of SOM by aggregates following a tillage event significantly increase turnover rates, resulting in a more rapid decline in stocks (Balesdent et al., 2000). This process is included in USSF. Nonetheless, in the simulations, the benefits of slower SOM turnover in the CNT treatment were negated by the higher input of above-ground residues under the CIT treatment, at least under the current humid climate at the study site. This is partly in agreement with the results of several long-term tillage experiments which found only small or no significant differences in total SOM stocks when comparing no-till with intensive tillage (e.g., Dimassi et al., 2013; Haddaway et al., 2017; Hermle et al., 2008; Martínez et al., 2016; Schulz et al., 2014).

Water balance

The annual water balance of the baseline simulations is shown in Table 5. The CNT treatment reduced evaporation by 14.8 cm yr^{-1} (- 65 %) and runoff by 2.4 cm yr^{-1} (- 97 %) and showed higher infiltration rates compared to the CIT treatment. Consequently, percolation rates were increased by up to 17.3 cm yr^{-1} (+ 34 %) in CNT. Transpiration did not differ between the treatments, as water was not a limiting factor (relative transpiration was near 100 % in all years).

In the model, the occurrence of surface runoff first depends on the infiltration capacity of the soil and subsequently the ponding capacity. The infiltration capacity is largely dependent on the saturated hydraulic conductivity of the topsoil, while the ponding capacity is determined by the amount of surface residues and only affects the fate of ponded water. As a consequence, the infiltration capacity played a much larger role in the generation of surface runoff than the ponding capacity.

The infiltration capacity of the topsoil was generally larger under CNT than CIT, leading to quicker infiltration and less ponding. A larger volume of stable bio-macroporosity under the CNT treatment was simulated, which permanently increased the saturated hydraulic conductivity near the soil surface to the point where after 2 years, virtually any precipitation immediately infiltrated into the soil. In the CIT treatment, tillage temporarily increased the macroporosity, but this was quickly lost to subsequent consolidation within 2 to 3 months, leading to low saturated hydraulic conductivities and infiltration capacities throughout most of the year. This reflects that tillage reduces soil aggregate stability and facilitates surface crusting, making recently tilled soils prone to rapid surface sealing and consolidation (Strudley et al., 2008). While previous experimental studies are inconsistent in their results (Blanco-Canqui et al., 2017), the simulation results agree with those of, e.g., Stone & Schlegel (2010), who associated higher infiltration rates with no-till compared to other tillage systems.

Crop residues on the soil surface are able to reduce evaporative water losses from the soil by shading and acting as a physical barrier to vapor fluxes (Hatfield et al., 2001). Other models predict a decrease of 5 - 40 % in evaporation under mulched conditions (Wang et al., 2021; Souza et al., 2022). The simple approach chosen in this model may therefore underestimate actual soil evaporation under residue cover.

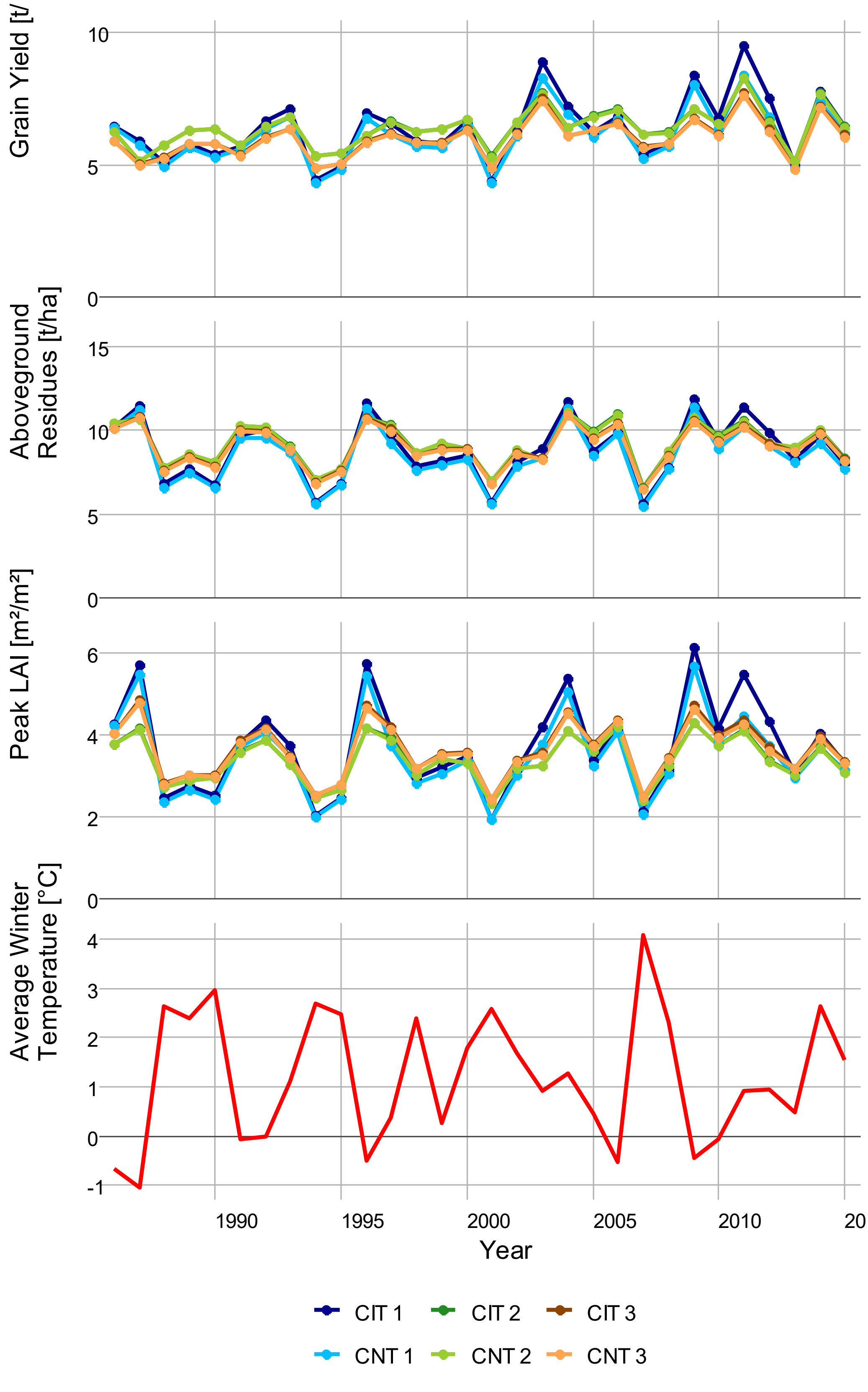

Figure 1: Simulated yearly grain harvest [t ha^{-1}], above-ground residues [t ha^{-1}], and peak LAI [m^2 m^{-2}] for the 3 final parameter sets and both treatments (CIT/CNT), as well as the mean winter temperatures (Dec-Feb) [°C] during the baseline period (1985-2015).

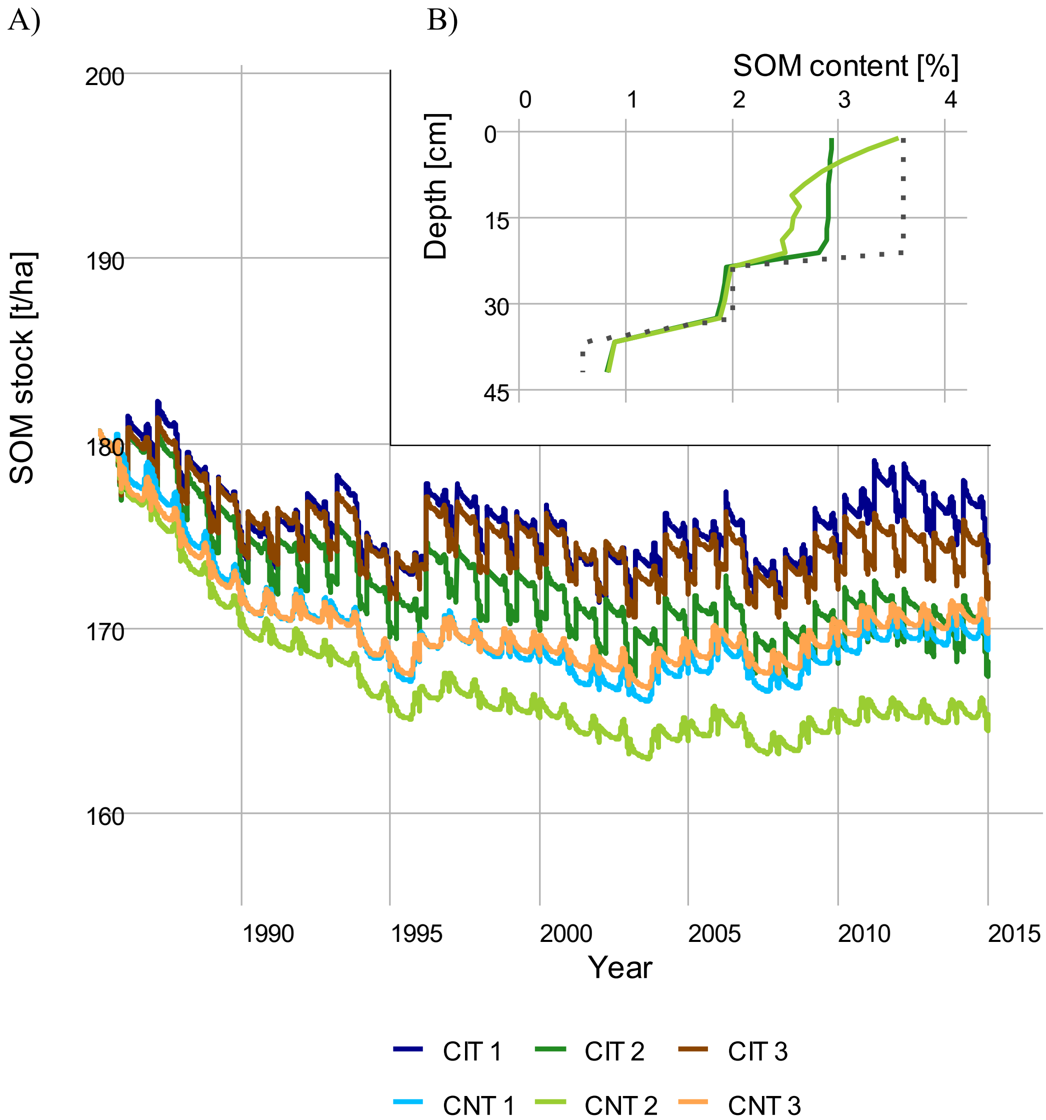

Figure 2: A) Simulated SOM stocks [t ha^{-1}] for the 3 final parameter sets and both treatments (CIT/CNT) during the baseline period (1985-2015). B) Example vertical distribution of gravimetric SOM content [%] at the end of the baseline period (2015), for parameter set 2. The dotted line represents the initial distribution (1985).

Table 4: Above-ground residue and SOM Balance during the baseline period (1986-2015), averaged over the 3 parameter sets

	$[t\ ha^{-1}\ yr^{-1}]$	CIT	CNT
Surface residues	Total above-ground shoot residues	+ 9.08	+ 8.95
	Residue harvest (export)	- 3.18	- 3.13
	Net surface crop residue return	*+ 5.90*	*+ 5.82*
	Tillage incorporation	- 2.88	-
	Bio-incorporation	- 1.06	- 2.03
	Total surface residue incorporation	*- 3.94*	*- 2.03*
	Surface residue respiration	- 1.96	- 3.77
	Change in surface residue stock	**± 0.00**	**+ 0.02**
SOM	**Root biomass & exudates**	+ 3.77	+ 3.77
	Total above-ground input	+ 3.94	+ 2.03
	Total input	*+ 7.71*	*+ 5.80*
	SOM Mineralization	- 7.92	- 6.21
	Change in SOM stock	**- 0.21**	**- 0.40**
	Error	-1.2×10^{-11}	1.6×10^{-11}

Table 5: Annual water balance during the baseline period (here: 01.08.1986 - 31.07.2015), averaged over the 3 parameter sets

[cm yr^{-1}]	**CIT**	**CNT**
Precipitation	103.6	103.6
Runoff	2.5	0.1
Evaporation	22.9	8.1
Transpiration	27.4	27.0
Percolation	51.0	68.3
Storage change	*- 0.1*	*+ 0.1*

3.3 Future climate scenarios

In total, 36 simulations were carried out for 2 SSPs, 3 different climate models (Table 2), 2 tillage systems and the 3 selected crop parameter sets (Table 3) .Figure 3 shows the yearly mean air temperature, grain yield and SOM stocks simulated with USSF for each scenario, averaged over the 3 crop parameter sets.

The climate projections predict an increase in annual mean temperature of between 1.2 and 8.0°C by 2090, depending on the SSP and climate model. Simultaneously, simulated grain yields decrease in most scenarios, with lower yields corresponding to higher temperatures. Only in the coolest of the six climate projections did grain yields remain stable, at an average of 7.3 t ha^{-1}, whereas in the hottest scenario, they decreased to 2.5 t ha^{-1}. The tillage system did not affect yields significantly.

SOM stocks declined in all future scenarios, again, with a steeper decline under hotter conditions. However, after a period of 15-35 years, the CNT treatment was able to consistently sustain higher SOM stocks than the tilled treatment. The differences between the two treatments were larger in the hotter climate projections.

Figure 4 shows the annual soil water balance (2061-2090) for 3 contrasting climate scenarios under the CIT and CNT treatments. Large differences can be observed between the different climate scenarios, especially concerning annual transpiration and evaporation rates. Evapotranspiration rates increased with higher temperatures, while percolation was reduced. Meanwhile, transpiration rates were very low in the hotter climate, but soil evaporation strongly increased. It must be noted that there was no drought stress affecting the crops (relative transpiration was near 100%), but leaf area and therefore potential transpiration rates were very low. The CNT treatment reduced surface runoff and evaporation in all climate scenarios, whereas percolation rates increased, compared to CIT. This effect was strongest under the cooler climatic conditions, where evaporation was reduced by up to 12.2 cm yr^{-1} (- 47 %).

As was already found in the baseline scenario, the low yields are a consequence of a shifting phenology due to higher temperatures, shortening the growth period of the crop. The resulting lack of crop residues limits the input of organic matter to the soil, while increasing temperatures accelerated mineralization rates. However, unlike in the baseline scenario, under future climate conditions, the CNT treatment was able to mitigate some of the SOM losses. In the model, the two governing mechanisms preserving SOM in the CNT treatment are the protection of SOM in the micropore region and thermal regulation through surface residue cover. Both these factors are able to slow SOM turnover rates, especially under hot conditions (Turmel et al., 2015; Verhulst et al., 2010). Several long-term experimental studies have therefore shown the positive effects of no-till practices on SOM stocks under the current climate in mediterranean region (Francaviglia et al., 2017), whereas the effects are generally weak in cooler, temperate regions (Hermle et al., 2008; Ogle et al., 2005; Palm et al., 2014; Scopel et al., 2013; Verhulst et al., 2010). This however suggests that, in the long run, no-till practices could have the potential to preserve SOM also in cooler regions of Europe when temperatures are rising. This would coincide with the simulation results for the baseline and future climate conditions.

A low crop canopy cover in the future scenarios combined with increased air temperatures led to high unproductive water loss through soil evaporation. This could partially be alleviated by surface residue cover in the CNT treatment. However, as this effect is dependent on the amount of produced crop residues, its effectiveness was reduced in the hot climate scenarios due to poor crop growth (Araya et al., 2024; Unger et al., 1991). Surface runoff could also be lowered under the CNT treatment, as the non-tilled soils maintained a higher macroporosity in the topsoil and the therefore higher infiltrability than the tilled soils. The CNT system was able to conserve water that would benefit root water availability and increase transpiration under a closed canopy (Page et al., 2019). Under the simulated conditions however, this increased percolation instead, which benefitted groundwater recharge rates.

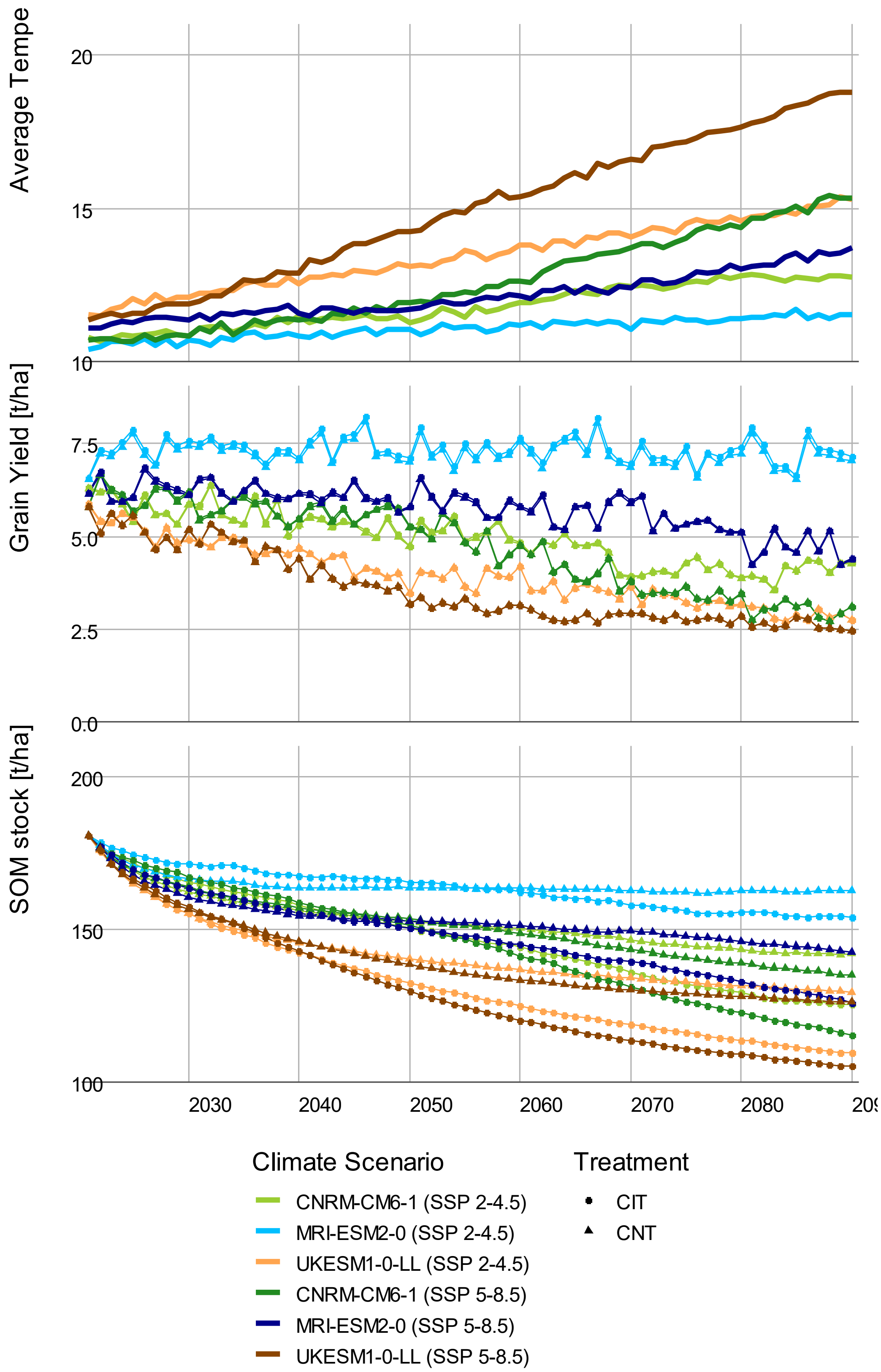

Figure 3: Average annual temperatures [°C] (2020-2090) for 2 SSPs and 3 climate models; simulated development of average grain yields [t ha^{-1}] and SOM stocks [t ha^{-1}] for both tillage treatments.

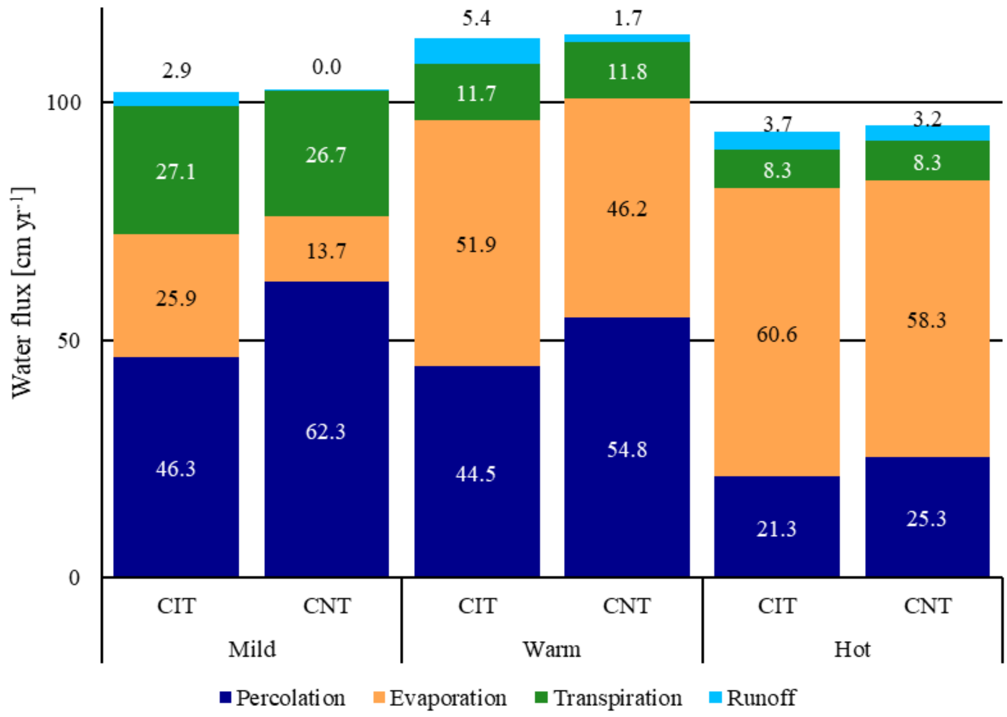

Figure 4: 30-year average annual soil water balance (2061-2090) for 3 different climate scenarios (mild = MRI-ESM2-0 (SSP 2-4.5); warm = CNRM-CM6-1 (SSP 5-8.5); hot = UKESM1-0-LL (SSP 5-8.5)) and 2 tillage systems

3.4 Model limitations and future development

While USSF provides a comprehensive collection of model functions for most relevant processes, certain potentially important mechanisms are yet being neglected or strongly simplified. Future model development should address the following areas:

- *Residue module*:
  The here introduced residue module was designed based on existing models but represents a strong simplification of real-world processes. Furthermore, some introduced parameters such as the retained fraction f_{ret} and the maximum decomposition rate k_{res} are both uncertain and highly dependent on the substrate. While the module produced plausible results, rigorous testing against experimental results needs to be conducted to assess its accuracy. Although more elaborate, physics-based models could have been used (e.g., Tadiello et al., 2023; Thorburn et al., 2001; Wang et al., 2021), this very simple approach was chosen due to limited information on residue amounts or properties.

- *Photoperiodism*:
  As discussed earlier, the currently employed phenology model may not be suited for simulating crop development in a warming climate and should be adjusted to include a photoperiod response function (e.g., Ceglar et al., 2019; Wang & Engel, 1998).

- *Nutrient cycling:*
  Nutrient cycling and feedback to crop growth is not part of the model, which in reality is influenced by SOM contents (Palm et al., 2014; Lal, 2015). This limits the applicability of USSF to simulate crop yields in farming systems with low nutrient inputs and might neglect positive influences of SOM conservation on soil fertility (Jarvis et al., 2024).

- *CO_2 fertilization:*
  While subject to high uncertainty, wheat yields in central and northern Europe are generally expected to increase due to rising levels of atmospheric CO_2 promoting plant growth (European Commission, 2020a; Faye et al., 2023). However, CO_2 concentrations are not currently affecting crop growth in USSF, which may therefore underestimate yield and residue biomass production in future climate and emission scenarios.

- *Traffic compaction:*
  Wheel traffic significantly increases the bulk density and consequently decreases porosity and infiltrability of soils (Godwin et al., 2015). This is currently not included in USSF and may for example lead to an underestimation of surface runoff in both treatments.

4. Conclusion

This study aimed to enhance the understanding of how different tillage and residue management practices influence soil quality, crop performance, and the water balance under current and future climate conditions in temperate Europe. Through the adaptation of the USSF model to include a crop residue module, this work provided insights into the long-term implications of two different tillage and residue management systems in a warming climate for a site in Switzerland.

Baseline simulations under current climate conditions showed that CNT improved the soil water balance, reducing surface runoff and conserving soil moisture compared to CIT. However, total SOM stocks were slightly lower under CNT, due to reduced input of above-ground residues. Crop yields did not differ between the tillage systems, potentially due to the model's limitations in accounting further soil management effects on crop growth, such as nutrient cycling, traffic compaction, or weeds.

Future climate scenarios projected a substantial decline in crop yields under hot conditions. This was mainly caused by an accelerated crop development associated with the applied phenology module, resulting in a much shorter growth period which may not reflect realistic conditions. Despite this, CNT systems demonstrated great potential to mitigate some of the adverse impacts of climate change, particularly by maintaining higher SOM stocks and conserving soil moisture.

This suggests that no-till practices, together with adequate residue management, could be a promising strategy for sustaining soil quality in the face of climate change. However, further model development and testing is needed to better predict the long-term dynamics of yields.

References

Agroscope. (2021). Farming System and Tillage Experiment – FAST alles im grünen Bereich. Agroscope. https://www.agroscope.admin.ch/agroscope/de/home/themen/umwelt-ressourcen/monitoring-analytik/langzeitversuche/fast.html

Andrén, O., & Kätterer, T. (1997). ICBM: The Introductory Carbon Balance Model for Exploration of Soil Carbon Balances. Ecological Applications, 7(4), 1226–1236. https://doi.org/10.2307/2641210.

Araya, T., Ochsner, T. E., Mnkeni, P. N. S., Hounkpatin, K. O. L., & Amelung, W. (2024). Challenges and constraints of conservation agriculture adoption in smallholder farms in sub-Saharan Africa: A review. International Soil and Water Conservation Research, S2095633924000200. https://doi.org/10.1016/j.iswcr.2024.03.001

Balesdent, J., Chenu, C., & Balabane, M. (2000). Relationship of soil organic matter dynamics to physical protection and tillage. Soil and Tillage Research, 53(3–4), 215–230. https://doi.org/10.1016/S0167-1987(99)00107-5

Beven, K., & Binley, A. (1992). The future of distributed models: Model calibration and uncertainty prediction. Hydrological Processes, 6(3), 279–298. https://doi.org/10.1002/hyp.3360060305

Blanco-Canqui, H., Wienhold, B. J., Jin, V. L., Schmer, M. R., & Kibet, L. C. (2017). Long-term tillage impact on soil hydraulic properties. Soil and Tillage Research, 170, 38–42. https://doi.org/10.1016/j.still.2017.03.001

Brooks, R. H., & Corey, A. T. (1964). Hydraulic properties of porous media. Colorado State University [Hydrology and Water Resources Program].

Ceglar, A., Črepinšek, Z., Kajfež-Bogataj, L., & Pogačar, T. (2011). The simulation of phenological development in dynamic crop model: The Bayesian comparison of different methods. Agricultural and Forest Meteorology, 151(1), 101–115. https://doi.org/10.1016/j.agrformet.2010.09.007

Ceglar, A., Van Der Wijngaart, R., De Wit, A., Lecerf, R., Boogaard, H., Seguini, L., Van Den Berg, M., Toreti, A., Zampieri, M., Fumagalli, D., & Baruth, B. (2019). Improving WOFOST model to simulate winter wheat phenology in Europe: Evaluation and effects on yield. Agricultural Systems, 168, 168–180. https://doi.org/10.1016/j.agsy.2018.05.002

Copernicus Climate Change Service. (2021). CMIP6 predictions underpinning the C3S decadal prediction prototypes [Dataset]. ECMWF. https://doi.org/10.24381/CDS.C866074C

Couchenev, E., Kätterer, T., Meurer, K. H. E., & Jarvis, N. (2024). Improving the sustainability of arable cropping systems by modifying root traits: A modelling study for winter wheat. European Journal of Soil Science, 75(4), e13524. https://doi.org/10.1111/ejss.13524

Craufurd, P. Q., & Wheeler, T. R. (2009). Climate change and the flowering time of annual crops. Journal of Experimental Botany, 60(9), 2529–2539. https://doi.org/10.1093/jxb/erp196

Dimassi, B., Cohan, J.-P., Labreuche, J., & Mary, B. (2013). Changes in soil carbon and nitrogen following tillage conversion in a long-term experiment in Northern France. Agriculture, Ecosystems & Environment, 169, 12–20. https://doi.org/10.1016/j.agee.2013.01.012

EEA (with Jacobs, C., Berglund, M., Kurnik, B., Dworak, T., Marras, S., Mereu, V., & Michetti, M.). (2019). Climate change adaptation in the agriculture sector in Europe. Publications Office of the European Union. doi.org/10.2800/537176

European Commission. (2020a). Analysis of climate change impacts on EU agriculture by 2050: JRC PESETA IV project : Task 3. Publications Office. https://data.europa.eu/doi/10.2760/121115

European Commission. (2020b). Caring for soil is caring for life: Ensure 75% of soils are healthy by 2030 for food, people, nature and climate : report of the Mission board for Soil health and food. Publications Office. https://data.europa.eu/doi/10.2777/821504

FAO. (2017). Voluntary Guidelines for Sustainable Soil Management. Food and Agriculture Organization of the United Nations. http://www.fao.org/3/a-i6874e.pdf

Faye, B., Webber, H., Gaiser, T., Müller, C., Zhang, Y., Stella, T., Latka, C., Reckling, M., Heckelei, T., Helming, K., & Ewert, F. (2023). Climate change impacts on European arable crop yields: Sensitivity to assumptions about rotations and residue management. European Journal of Agronomy, 142, 126670. https://doi.org/10.1016/j.eja.2022.126670

Francaviglia, R., Di Bene, C., Farina, R., & Salvati, L. (2017). Soil organic carbon sequestration and tillage systems in the Mediterranean Basin: A data mining approach. Nutrient Cycling in Agroecosystems, 107(1), 125–137. https://doi.org/10.1007/s10705-016-9820-z

Godwin, R., Misiewicz, P., White, D., Smith, E., Chamen, T., Galambošová, J., & Stobart, R. (2015). Results From Recent Traffic Systems Research And The Implications For Future Work. Acta Technologica Agriculturae, 18(3), 57–63. https://doi.org/10.1515/ata-2015-0013

Gonzalez-Sosa, E., Braud, I., Thony, J. L., Vauclin, M., & Calvet, J. C. (2001). Heat and water exchanges of fallow land covered with a plant-residue mulch layer: A modelling study using the three year MUREX data set. Journal of Hydrology, 244(3–4), 119–136. https://doi.org/10.1016/S0022-1694(00)00423-6

Güntner, A., Olsson, J., Calver, A., & Gannon, B. (2001). Cascade-based disaggregation of continuous rainfall time series: The influence of climate. Hydrology and Earth System Sciences, 5(2), 145–164. https://doi.org/10.5194/hess-5-145-2001

Haddaway, N. R., Hedlund, K., Jackson, L. E., Kätterer, T., Lugato, E., Thomsen, I. K., Jørgensen, H. B., & Isberg, P.-E. (2017). How does tillage intensity affect soil organic carbon? A systematic review. Environmental Evidence, 6(1), 30. https://doi.org/10.1186/s13750-017-0108-9

Hatfield, J. L., Sauer, T. J., & Prueger, J. H. (2001). Managing Soils to Achieve Greater Water Use Efficiency: A Review. Agronomy Journal, 93(2), 271–280. https://doi.org/10.2134/agronj2001.932271x

Hermle, S., Anken, T., Leifeld, J., & Weisskopf, P. (2008). The effect of the tillage system on soil organic carbon content under moist, cold-temperate conditions. Soil and Tillage Research, 98(1), 94–105. https://doi.org/10.1016/j.still.2007.10.010

IPCC. (2023). Climate Change 2023: Synthesis Report (First). Intergovernmental Panel on Climate Change (IPCC). https://doi.org/10.59327/IPCC/AR6-9789291691647

Jarvis, N. (2008). Near-Saturated Hydraulic Properties of Macroporous Soils. Vadose Zone Journal, 7(4), 1302–1310. https://doi.org/10.2136/vzj2008.0065

Jarvis, N., Coucheney, E., Lewan, E., Klöffel, T., Meurer, K. H. E., Keller, T., & Larsbo, M. (2024). Interactions between soil structure dynamics, hydrological processes, and organic matter cycling: A new soil-crop model. European Journal of Soil Science, 75(2), e13455. https://doi.org/10.1111/ejss.13455

Kroes, J. G., van Dam, J. C., Bartholomeus, R. P., Groenendijk, P., Heinen, M., Hendriks, R. F. A., Mulder, H. M., Supit, I., & van Walsum, P. E. V. (2017). SWAP version 4. Wageningen Environmental Research. https://doi.org/10.18174/416321

Lal, R. (2015). Restoring Soil Quality to Mitigate Soil Degradation. Sustainability, 7(5), 5875–5895. https://doi.org/10.3390/su7055875

Martínez, I., Chervet, A., Weisskopf, P., Sturny, W. G., Etana, A., Stettler, M., Forkman, J., & Keller, T. (2016). Two decades of no-till in the Oberacker long-term field experiment: Part I. Crop yield, soil organic carbon and nutrient distribution in the soil profile. Soil and Tillage Research, 163, 141–151. https://doi.org/10.1016/j.still.2016.05.021

MeteoSwiss. (2024). Federal Office of Meteorology and Climatology MeteoSwiss. https://www.meteoswiss.admin.ch/

Meurer, K. H. E., Chenu, C., Coucheney, E., Herrmann, A. M., Keller, T., Kätterer, T., Nimblad Svensson, D., & Jarvis, N. (2020). Modelling dynamic interactions between soil structure and the storage and turnover of soil organic matter. Biogeosciences, 17(20), 5025–5042. https://doi.org/10.5194/bg-17-5025-2020

Mualem, Y. (1976). A new model for predicting the hydraulic conductivity of unsaturated porous media. Water Resources Research, 12(3), 513–522. https://doi.org/10.1029/WR012i003p00513

Nash, J. E., & Sutcliffe, J. V. (1970). River flow forecasting through conceptual models part I - A discussion of principles. Journal of Hydrology, 10(3), 282–290. https://doi.org/10.1016/0022-1694(70)90255-6

Ogle, S. M., Breidt, F. J., & Paustian, K. (2005). Agricultural management impacts on soil organic carbon storage under moist and dry climatic conditions of temperate and tropical regions. Biogeochemistry, 72(1), 87–121. https://doi.org/10.1007/s10533-004-0360-2

Olsson, J. (1998). Evaluation of a scaling cascade model for temporal rainfall disaggregation. Hydrology and Earth System Sciences, 2(1), 19–30. https://doi.org/10.5194/hess-2-19-1998

Page, K. L., Dang, Y. P., Dalal, R. C., Reeves, S., Thomas, G., Wang, W., & Thompson, J. P. (2019). Changes in soil water storage with no-tillage and crop residue retention on a Vertisol: Impact on productivity and profitability over a 50 year period. Soil and Tillage Research, 194, 104319. https://doi.org/10.1016/j.still.2019.104319

Palm, C., Blanco-Canqui, H., DeClerck, F., Gatere, L., & Grace, P. (2014). Conservation agriculture and ecosystem services: An overview. Agriculture, Ecosystems & Environment, 187, 87–105. https://doi.org/10.1016/j.agee.2013.10.010

Prechsl, U. E., Wittwer, R., Van Der Heijden, M. G. A., Lüscher, G., Jeanneret, P., & Nemecek, T. (2017). Assessing the environmental impacts of cropping systems and cover crops: Life cycle assessment of FAST, a long-term arable farming field experiment. Agricultural Systems, 157, 39–50. https://doi.org/10.1016/j.agsy.2017.06.011

Schulz, F., Brock, C., Schmidt, H., Franz, K.-P., & Leithold, G. (2014). Development of soil organic matter stocks under different farm types and tillage systems in the Organic Arable Farming Experiment Gladbacherhof. Archives of Agronomy and Soil Science, 60(3), 313–326. https://doi.org/10.1080/03650340.2013.794935

Scopel, E., Triomphe, B., Affholder, F., Da Silva, F. A. M., Corbeels, M., Xavier, J. H. V., Lahmar, R., Recous, S., Bernoux, M., Blanchart, E., De Carvalho Mendes, I., & De Tourdonnet, S. (2013). Conservation agriculture cropping systems in temperate and tropical conditions, performances and impacts. A review. Agronomy for Sustainable Development, 33(1), 113–130. https://doi.org/10.1007/s13593-012-0106-9

Sellar, A. A., Jones, C. G., Mulcahy, J. P., Tang, Y., Yool, A., Wiltshire, A., O’Connor, F. M., Stringer, M., Hill, R., Palmieri, J., Woodward, S., De Mora, L., Kuhlbrodt, T., Rumbold, S. T., Kelley, D. I., Ellis, R., Johnson, C. E., Walton, J., Abraham, N. L., … Zerroukat, M. (2019). UKESM1: Description and Evaluation of the U.K. Earth System Model. Journal of Advances in Modeling Earth Systems, 11(12), 4513–4558. https://doi.org/10.1029/2019MS001739

Semenov, M., & Barrow, E. (2002). LARS-WG A Stochastic Weather Generator for Use in Climate Impact Studies. https://sites.google.com/view/lars-wg/

Souza, R., Jha, A., & Calabrese, S. (2022). Quantifying the hydrological impact of soil mulching across rainfall regimes and mulching layer thickness. Journal of Hydrology, 607, 127523. https://doi.org/10.1016/j.jhydrol.2022.127523

Stone, L. R., & Schlegel, A. J. (2010). Tillage and Crop Rotation Phase Effects on Soil Physical Properties in the West-Central Great Plains. Agronomy Journal, 102(2), 483–491. https://doi.org/10.2134/agronj2009.0123

Strudley, M., Green, T., & Ascoughii, J. (2008). Tillage effects on soil hydraulic properties in space and time: State of the science. Soil and Tillage Research, 99(1), 4–48. https://doi.org/10.1016/j.still.2008.01.007

Tadiello, T., Gabbrielli, M., Botta, M., Acutis, M., Bechini, L., Ragaglini, G., Fiorini, A., Tabaglio, V., & Perego, A. (2023). A new module to simulate surface crop residue decomposition: Description and sensitivity analysis. Ecological Modelling, 480, 110327. https://doi.org/10.1016/j.ecolmodel.2023.110327

Thorburn, P. J., Probert, M. E., & Robertson, F. A. (2001). Modelling decomposition of sugar cane surface residues with APSIM–Residue. Field Crops Research, 70(3), 223–232. https://doi.org/10.1016/S0378-4290(01)00141-1

Turmel, M.-S., Speratti, A., Baudron, F., Verhulst, N., & Govaerts, B. (2015). Crop residue management and soil health: A systems analysis. Agricultural Systems, 134, 6–16. https://doi.org/10.1016/j.agsy.2014.05.009

Unger, P. W., Stewart, B. A., Parr, J. F., & Singh, R. P. (1991). Crop residue management and tillage methods for conserving soil and water in semi-arid regions. Soil and Tillage Research, 20(2–4), 219–240. https://doi.org/10.1016/0167-1987(91)90041-U

Verhulst, N., Govaerts, B., Verachtert, E., Castellanos-Navarrete, A., Mezzalama, M., Wall, P. C., Chocobar, A., Deckers, J., & Sayre, K. D. (2010). Conservation Agriculture, Improving Soil Quality for Sustainable Production Systems? In R. Lal & B. A. Stewart (Eds.), Food Security and Soil Quality (0 ed., pp. 137–208). CRC Press. https://doi.org/10.1201/EBK1439800577-7

Voldoire, A., Saint-Martin, D., Sénési, S., Decharme, B., Alias, A., Chevallier, M., Colin, J., Guérémy, J. -F., Michou, M., Moine, M. -P., Nabat, P., Roehrig, R., Salas Y Mélia, D., Séférian, R., Valcke, S., Beau, I., Belamari, S., Berthet, S., Cassou, C., … Waldman, R. (2019). Evaluation of CMIP6 DECK Experiments With CNRM-CM6-1. Journal of Advances in Modeling Earth Systems, 11(7), 2177–2213. https://doi.org/10.1029/2019MS001683

Wang, E., & Engel, T. (1998). Simulation of phenological development of wheat crops. Agricultural Systems, 58(1), 1–24. https://doi.org/10.1016/S0308-521X(98)00028-6

Wang, Z., Thapa, R., Timlin, D., Li, S., Sun, W., Beegum, S., Fleisher, D., Mirsky, S., Cabrera, M., Sauer, T., Reddy, V. R., Horton, R., & Tully, K. (2021). Simulations of Water and Thermal Dynamics for Soil Surfaces With Residue Mulch and Surface Runoff. Water Resources Research, 57(11), e2021WR030431. https://doi.org/10.1029/2021WR030431

Watroba, M., & Levy Häner, L. (2021). Winterweizen 2020 – Sortenversuche unter Biobedingungen (401; Agroscope Transfer). Agroscope. https://doi.org/10.34776/AT401GF

Wheeler, T. R., Batts, G. R., Ellis, R. H., Hadley, P., & Morison, J. I. L. (1996). Growth and yield of winter wheat crops in response to CO2 and temperature. The Journal of Agricultural Science, 127(1), 37–48. https://doi.org/10.1017/S0021859600077352

Wittwer, R. A., Dorn, B., Jossi, W., & Van Der Heijden, M. G. A. (2017). Cover crops support ecological intensification of arable cropping systems. Scientific Reports, 7(1), 41911. https://doi.org/10.1038/srep41911

Yukimoto, S., Kawai, H., Koshiro, T., Oshima, N., Yoshida, K., Urakawa, S., Tsujino, H., Deushi, M., Tanaka, T., Hosaka, M., Yabu, S., Yoshimura, H., Shindo, E., Mizuta, R., Obata, A., Adachi, Y., & Ishii, M. (2019). The Meteorological Research Institute Earth System Model Version 2.0, MRI-ESM2.0: Description and Basic Evaluation of the Physical Component. Journal of the Meteorological Society of Japan. Ser. II, 97(5), 931–965. https://doi.org/10.2151/jmsj.2019-051

Popular science summary

European soils are in poor condition, leading to the exploration of measures like reduced tillage and residue retention for their ability prevent soil degradation. These practices, collectively known as conservation agriculture, aim to make farming more sustainable and resilient to climate change. However, traditional crop models often neglect changes in soil properties over time, limiting their applicability to predict the effectiveness of conservation agriculture in the face of climate change.

This study uses a novel model called the Uppsala model of Soil Structure and Function to examine the long-term effects of conservation agriculture on soil structure, soil organic matter (SOM), the water balance, and winter wheat yields in temperate Europe, under both current and future climates. Two farming systems are compared: conventional tillage, in which the soil is ploughed and crop residues incorporated, and no-till, where the soil is left undisturbed and crop residues remain as a protective layer on the surface. The model was calibrated for a site in Switzerland and used to simulate recent climatic conditions using recorded data between 1985 and 2015, and subsequently applied to explore possible future developments under 18 future climate scenarios for 2020-2090.

The results showed that under current climate conditions, the no-till system reduced water losses through surface runoff and evaporation. However, this did not improve winter wheat yields since water availability was not limiting crop growth. After 30 years, SOM was slightly higher under conventional tillage due to more crop residues being mixed into the soil through tillage. In the future scenarios, hotter climate conditions led to shorter growing periods and causing drastic yield declines. This however is likely not a realistic prospect, but instead was caused by the application of a modelling approach that might not be suited to simulate warming climate. As a consequence of reduced biomass production and accelerated turnover of SOM the model predicted lower SOM levels in all scenarios. However, no-till farming maintained 14 % higher SOM on average than conventional tillage and conserved more soil moisture.

Thus, despite not being able to increase yields in this study, no-till showed potential to preserve soil function and mitigate some negative effects of climate change. This suggests that conservation agriculture could help protect European soils in the future, but further model improvements are needed to better predict long-term effects on crop yields.

Acknowledgements

I want to express my sincere gratitude to my supervisors from SLU, Nicholas Jarvis and Elsa Coucheney for their continuous help, guidance and patience, without which this endeavour would not have been possible. I further want to thank my co-supervisor Sebastian Gayler for his support. Many thanks also to my examiner Mats Larsbo and my opponent Yannic Janal for their careful feedback and suggestions. Lastly, I want to thank EJP Soil for the funding of the project and providing the necessary data for this thesis.

Appendix

Table A1: Soil profile description

Name:		FAST Blocks B-D, Soil Profile No UR266					
Location:		8153 Rümlang, Switzerland (N 47.4395°, E 8.5273°)					
Soil Type (Swiss):		Braunerde					
Soil Type (WRB):		Endostagnic Cambisol					
Depth [cm]	Horizon (Swiss)	Texture classes [%]			Rock fraction [%]	SOC content* [%]	pH [-]
		Sand	Silt	Clay			
0 - 22	Ahp	46.5	33.2	20.3	11	1.8	6
22 - 34	Aba,(x)	50.1	20.5	29.4	11	1.0	6.5
34 - 72	B(g),(x)	41.3	30.0	28.7	11	0.3	6.7
73 - 93	BCg	60.5	14.2	25.3	18	0.2	7.2
93 - 110	C					0.2	7.2

* SOC content = gravimetric soil organic carbon content

*Table A2: Default phenological parameter values for winter wheat. Vernalization parameters as described in Ceglar et al., 2018. *Default values of the SWAP model (Kroes et al., 2017). **Temperature sums derived from observational data.*

Vernalization		**Crop development**	
T_{v1} [°C]	-4*	T_b [°C]	0*
T_{v2} [°C]	3*		
T_{v3} [°C]	10*	$T_{sum(e)}$ [°C d]	70**
T_{v4} [°C]	17*	$T_{sum(a)}$ [°C d]	1200**
V_b [-]	8*	$T_{sum(m)}$ [°C d]	2000**
V_{sat} [-]	41*		

Table A3: Parameter descriptions and values used in the residue module

Parameter	Description	Value	Unit
$B_{res\,(ini)}$	Initial residue biomass	0.0235	g cm^{-2}
$\rho_{b\,(res)}$	Residue bulk density	0.025	g cm^{-3}
k_{res}	Maximum decomposition rate constant of surface residues	0.014	day^{-1}
$T_{opt\,(res)}$	Optimum air temperature for decomposition of surface residues	20	°C
f_{ret}	Fraction of residues retained as SOM (not respired) during decomposition	0.35	-
$f_{10\,cm}$	Fraction of organic matter bioincorporated above 10cm depth	0.70	-
α_{bio}	Rate of bioporosity generation per amount of surface residue	0.36	$m^3\ m^{-3}\ d^{-1}$ $(g\ cm^{-2})^{-1}$
τ_{a_0}	Minimum rate of bioporosity generation in the absence of surface residues	$25 \cdot 10^{-6}$	day^{-1}
$B_{res\,(crit)}$	Critical residue amount for full soil cover	0.03	g cm^{-2}
D_{res}	Thermal diffusivity of the residue layer	300	$cm^2\ day^{-1}$
β_{res}	Specific water holding capacity of crop residues	10	$cm^3\ g^{-1}$

Publishing and archiving

Approved students' theses at SLU are published electronically. As a student, you have the copyright to your own work and need to approve the electronic publishing. If you check the box for **YES**, the full text (pdf file) and metadata will be visible and searchable online. If you check the box for **NO**, only the metadata and the abstract will be visible and searchable online. Nevertheless, when the document is uploaded it will still be archived as a digital file. If you are more than one author, the checked box will be applied to all authors. You will find a link to SLU's publishing agreement here:

- https://libanswers.slu.se/en/faq/228318.

☒ YES, I/we hereby give permission to publish the present thesis in accordance with the SLU agreement regarding the transfer of the right to publish a work.

☐ NO, I/we do not give permission to publish the present work. The work will still be archived and its metadata and abstract will be visible and searchable.